Sensors & Actuators: A. Physical 381 (2025) 116038

Contents lists available at ScienceDirect

Sensors and Actuators: A. Physical

journal homepage: www.journals.elsevier.com/sensors-and-actuators-a-physical

Piezo-Ionic Actuator for Haptic Feedback

António Diogo André [a,b], Indrani Coondoo [c], Igor Bdikin [d,e], Vinaya Kumar K.B. [f], Rui M.R. Pinto [g], Pedro Martins [b,h], Majid Taghavi [a,i,*]

[a] Department of Bioengineering, Imperial College London, London, UK
[b] Institute of Science and Innovation in Mechanical and Industrial Engineering (INEGI), Porto, Portugal
[c] Department of Materials and Ceramic Engineering & CICECO - Aveiro Institute of Materials, University of Aveiro, Aveiro, Portugal
[d] Centre for Mechanical Technology and Automation (TEMA), Department of Mechanical Engineering, University of Aveiro, Aveiro, Portugal
[e] Intelligent Systems Associate Laboratory (LASI), Guimarães, Portugal
[f] Department of Electrical and Electronics Engineering, Birla Institute of Technology & Science Pilani K K Birla Goa Campus, Goa, India
[g] International Iberian Nanotechnology Laboratory (INL), Braga, Portugal
[h] Instituto de Investigación en Ingeniería de Aragón (i3A), Universidad de Zaragoza, Zaragoza, Spain
[i] School of Engineering and Materials Science, Queen Mary University of London, London, UK

ARTICLE INFO

Keywords:
PVDF
Piezoelectric actuator
Ionic actuator
Electromechanical response
Haptic feedback

ABSTRACT

Electroactive polymers have received substantial attention for actuation because of their muscle-like actuation behaviour. These polymers are typically studied under ionic and electric classes based on their fundamental response mechanisms. In this study, a hybrid piezo-ionic actuator is developed and characterised by its electromechanical response to analyse the piezo-ionic synergistic effect in a cantilever beam actuation design. The piezo-ionic actuator was developed using polyvinylidene fluoride (PVDF) combined with an [Pmim][TFSI] ionic liquid (IL) filler. The addition of IL into the PVDF network promotes the formation of electroactive phases (β and γ), consequently enhancing the electromechanical response of PVDF while maintaining the characteristic fast response time of piezo materials. The IL also plasticize the PVDF polymer and increases its conductivity which also causes the electrical parameters to vary with frequency. It results in higher dielectric loss, energy storage and hysteresis in PVDF/IL responses. To evaluate the actuator performance, the force generated by the hybrid actuator is measured and a finger sleeve is designed for haptic feedback analysis.

1. Introduction

Electroactive polymers capable of converting electrical energy into mechanical motion and vice versa [1], have received substantial attention for their applications across different sectors, including industry [2] and healthcare [3]. The soft nature of these polymers makes them ideal for lightweight actuation while offering straightforward and flexible design options [4]; although with limited output force [5,6]. These polymers are commonly classified into ionic and electric types based on their response mechanism [7]. In ionic actuators, the actuation response is caused by the displacement of ions within the polymer, typically requiring low voltages to trigger a mechanical response. In contrast, electric actuators respond to the electrical stimuli through the polarization of dipoles [8]. Ionic actuators are known for their slower response time and relatively lower force output, which can constrain their use in applications where minimal force is sufficient. For example, Heydt. et al. [9] and Ren et al. [10], used ionic actuators in the development of refreshable Braille display, and Hardy et al. demonstrated their application in drug delivery systems [11].

Piezoelectric materials, categorised under electric actuators, employ the converse piezoelectric effect, to alter their shape in response to electrical stimuli. Piezoelectric polymers, such as polyvinylidene fluoride (PVDF) known for its high piezoelectric constant among the polymers [12], demonstrate lower displacement when compared to ionic-based polymers [13,14,15]. However, their response is quicker, making the piezoelectric actuators ideal for high frequency and precision positioning tasks [16]. For example, it has been used in bimorph actuators for laser scanning actuation at high frequencies [17], ideal for high-speed manipulation as well as in haptics [18], and touch displays [19]). The actuation performance of PVDF is influenced directly by the presence of electroactive phases (β and γ), which are typically minimal in pure states [20]. These phases can be enhanced through a phase

* Corresponding author at: Department of Bioengineering, Imperial College London, London, UK.
E-mail address: m.taghavi@imperial.ac.uk (M. Taghavi).

https://doi.org/10.1016/j.sna.2024.116038
Received 24 August 2024; Received in revised form 21 October 2024; Accepted 6 November 2024
Available online 22 November 2024

transition, solvent casting, the addition of nucleating fillers or the development of new PVDF copolymers [21]. The incorporation of ionic liquid as nucleating fillers to enhance piezoelectricity has received interest, with studies comparing different types of ionic liquids in the composition [22,23,24], the porosity of the polymer [25], and embedded electrodes [26]. The inclusion of IL in the PVDF network can potentially have a synergistic effect on the actuation mechanism benefiting from both ionic and piezoelectric actuation principles. First, ionic liquids act as a plasticizer in the network, reducing Young's modulus of the actuator [22,27], thus enabling larger deformation for these actuators. Second, the inclusion of ionic liquids allows for ionic mobility and conductivity in the composite, decreasing the actuation voltage when compared to pure piezoelectric materials. The actuation behaviour of these hybrid piezo-ionic actuators, along with their hysteresis and durability, has not yet been thoroughly investigated. They are influenced by various factors, including the type of ionic liquids in the polymeric network, electrode composition, and fabrication parameters such as solvent and curing process. This work aims to address this gap by investigating the electromechanical properties and actuation performance of a PVDF-IL composite (Fig. 1) for potential haptic applications. Our material development process involves optimizing the fabrication process with a non-toxic solvent, dimethylsulfoxide (DMSO), and leveraging the thermoplasticity of the film for a straightforward heat-transfer printing technique to embed electrodes. We have based our studies on the 1-Methyl-3-propylimidazolium bis(trifluoromethylsulfonyl)imide ([PMIM][TFSI]) as the ionic liquid, which has been reported to significantly increase the crystallization of electroactive phases of PVDF, among various cations and anions studied [22,23]. Our mechanical characterization shows that this reduces the Young's modulus of the films by approximately tenfold compared to pure PVDF, confirming the plasticizing effect of IL [27], with the mean Young modulus of 144 MPa and a yield stress of σ_{Yield}=9 MPa.

2. Materials and methods

2.1. Actuation development

The PVDF/IL material was developed using a PVDF powder (Solef 6020 by SolvayLda), an ionic liquid(IL)(1-Methyl-3-propylimidazoliumbis (trifluoromethylsulfonyl)imide, [PMIM][TFSI], ≥ 99 %) from IoliTec-Ionic GmbH, and a polar non-toxic solvent to dissolve and mix PVDF with the IL, dimethylsulfoxide (DMSO, 99.9+% ACS) from Thermo Fisher Scientific.

The PVDF/IL films were prepared using the protocol outlined by André et al. [27]. First, DMSO and IL were mixed and after achieving a homogeneous mixture, PVDF was added to the solution. The ratio between the materials is 40 % w/w IL/PVDF and 12/88 % w/w PVDF/DMSO. The solution in a sealed beaker was stirred within a thermal bath maintained at 50ºC. Once a transparent and homogeneous solution was achieved, the mixture was poured onto a glass substrate. The wet film thickness was defined as 0.6 mm through the doctor blade technique (using an applicator, Proceq ZUA 2000). For total solvent evaporation, the wet film was taken into the oven, set at 85ºC to avoid the formation of pores [28], and to allow a better piezoelectric β phase crystallization [29]. Fig. 2a provides a schematic representation summarizing this fabrication process.

For voltage application, thin gold leaf sheets were laminated on both faces of the samples using a hot-press printing technique. PVDF/IL films were sandwiched between the gold sheets on the top and the bottom faces and compressed at 180ºC for 45 seconds (Fig. 2b). Fig. 2c shows the PVDF/IL film (with a thickness of 0.06 mm) both before and after the gold lamination step.

2.2. Electrical characterization

The capacitance (C) and ohmic resistance (R) of the PVDF/IL film were measured using an LCR meter (Agilent E4980A) across a frequency range of 20 Hz to 2 MHz and a voltage intensity (V_{AC}) of 1 V. Circular electrodes with a diameter of 5.3 mm were used on both faces of the samples for the measurements. Based on these results, we determined the real part of the relative permittivity (ε') using $\varepsilon' = \frac{C \cdot d}{\varepsilon_0 \cdot A}$ and AC conductivity (σ_{AC}) using $\sigma_{AC} = \frac{d}{R \cdot A}$ where d represents the thickness of the samples, ε_0 stands for the permittivity of vacuum (8.85×10^{-12} F/m) and A denotes the electrode area.

2.3. Electromechanical analysis

The piezoelectric constant (d_{33}) of the PVDF/IL composite was determined using the piezoresponse force microscopy (PFM) technique. Local piezoresponse and polarization switching spectroscopy of the PVDF/IL film were conducted with a commercial scanning probe microscope (Veeco Multimode Nanoscope IV microscope, Houghton, MI, USA). A conductive probe (NSG10/Pt, NT-MDT) with a spring constant of 14 N/m was used and the piezoresponse force microscopy out-of-plane images were scanned in the single frequency mode at 7.5 V and with a frequency of 35 kHz.

We studied the electromechanical responses of the PVDF/IL film samples cut in a rectangular shape (6×30 mm^2). The samples were displaced vertically in a cantilever beam configuration, constrained at the top end and free at the bottom end, where a laser was pointed for the measurements. For sinusoidal stimulations, we used input signals with frequencies of 0.11, 0.2, 1.1 and 2 Hz and voltages of 5, 10, 15 and 20 V_{pp} for the duration of 90 seconds. Actuation signals were generated by a function generator (Multicomp Pro MP750064) and the resultant

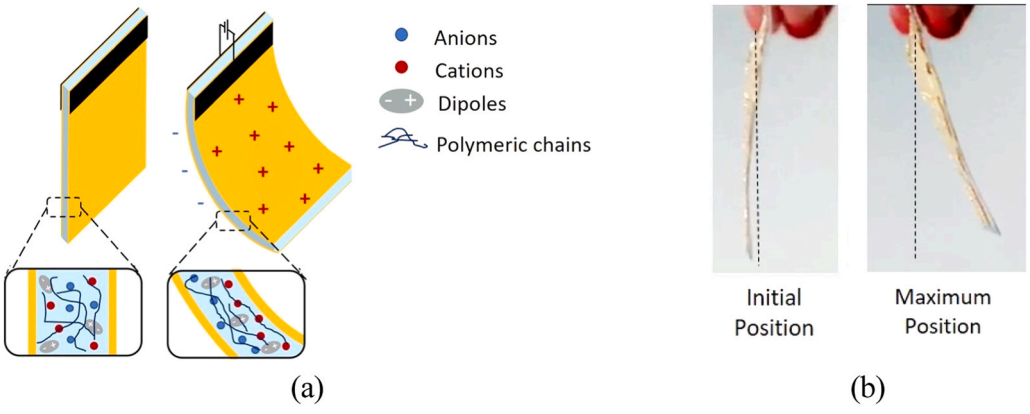

Fig. 1. The PVDF-IL film sandwiched between electrodes: (a) Schematic representing the actuation mechanism; (b) Movement of the sample under applied voltage (10 V, 0.05 Hz).

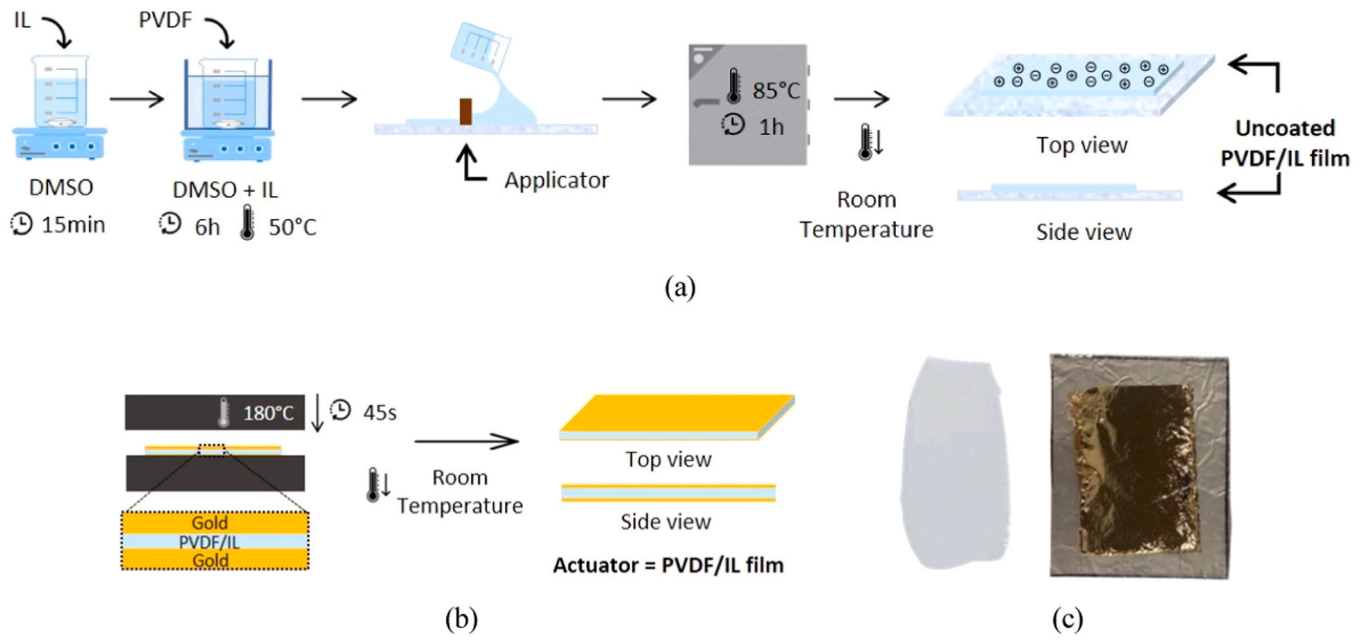

Fig. 2. Fabrication process: (a) Schematic illustration of PVDF/IL film development; (b) Gold-layer heat printing; (c) Photograph showing the uncoated sample (left) and gold-coated sample (right).

displacement was measured using a laser displacement meter (controller Keyence LK-G3001P + laser Keyence LK-G152) directed to the tip of the samples. Each PVDF/IL sample was tested once for a set of frequency and voltage. For analysis at 20 V, the mean of two sample measurements was used for each frequency due to higher movement variance in this voltage. We considered the first 15 peaks of each trial for the mean sine displacement ± standard deviation (STD) analysis, excluding the first and last peaks to ensure movement stability. The displacement at each peak (crest or trough) was regarded as the peak-to-peak amplitude.

We investigated the active displacement of the samples with a single square pulse per duration of 1, 5 and 10 seconds. Each pulse duration was applied at least 5 minutes apart to ensure complete relaxation of the samples, while the voltage amplitude was maintained at 10 V. This also includes phased displacement analysis, which reflects out-of-phase rising or relaxation of the samples. Each case was tested with 5 pulses.

The rising speed, from the time of pulse application to the moment of maximum displacement within the pulse duration, and the relaxation speed, calculated from the end of the pulse to the minimum position of the samples, were investigated at different pulse amplitudes (2.5, 5, 7.5 and 10 V). These signals were applied to 3 samples in single pulses lasting for 1 s each. Additionally, the reversal motion speed was determined by applying a bipolar square pulse 9 times, distributed across 3 samples with at least 5-minute intervals between each pulse. This measurement indicates how quickly the sample returns to its initial position after the polarity of the signal is inverted. The square waves had a period (T) of 2 s and a voltage amplitude of 20 V_{pp}.

To investigate the performance of the samples under continuous cyclic stimulation, we applied periodic sine waveforms at 0.2 Hz and input voltages of 10 V_{pp} to the actuators for 25 minutes.

The actuation force was investigated using a setup where the actuators displaced against a compression spring with a spring constant of k = 0.0294 N/mm (5055, Misumi) during the first half of the biphasic square pulse. A total of 9 pulses, each with a voltage of 20 V_{pp} and a period (T) of 2 were applied. The contact force between the actuator and spring is equal to the compression force of the spring, which is directly proportional to the decrease in length of the spring (x) in Hooke's law: $F = -k \cdot x$

All data was collected using a data acquisition device (National Instruments USB-6001) and subsequently processed in MATLAB.

3. Results and discussion

Fig. 3a shows the real part of the relative permittivity (ε') and conductivity σ_{AC} measured for the PVDF-IL film. The data shows that ε' decreases with the frequency, from $1.83x10^{3}$±156.96 to 2.91±0.11, while the electrical conductivity (σ_{AC}), increases with frequency from.$86x10^{-6}$±$2.37x10^{-7}$ S/m to $2.50x10^{-4}$±$5.80x10^{-6}$ S/m. These trends are consistent with those reported in the literature for hybrid piezo-ionic materials [22,30]. This behaviour is attributed to the presence of IL in the polymeric matrix. In contrast, pure PVDF does not exhibit such frequency dependence with σ_{AC} remaining at 1.61×10^{-08} S/m and ε' at 10, considering a frequency range of 100 Hz - 1 MHz [22]. Higher values of σ_{AC} represent higher electrical losses in the piezoelectric film, while higher values of ε' indicate the material's enhanced capability to store electrical energy [31].

Fig. 3b shows the topography of the PVDF/IL film obtained from the scanning of the surface, showing an average roughness of ≈120 nm. This measurement employs the standard contact mode atomic force microscopy (AFM) to reveal the topography of the samples. In comparison, the pure PVDF films show a lower average roughness of around 30 nm (see supplementary figure 1a). The increased roughness in the PVDF/IL films can be attributed to the incorporation of the ionic liquid, which induces greater surface irregularities Moreover, we conducted PFM measurements to evaluate the local piezoelectric response of the PVDF/IL and PVDF sample. This technique is based on the standard contact mode AFM setup, in which the cantilever and the tip are electrically conductive, and an alternating voltage is applied to the tip, evaluating the electromechanical properties in addition to the sample topography. Fig. 3c shows the nanoscale topography of the PVDF/IL film through the PFM technique, with the correspondng topography for the pure PVDF samples shown in supplementary figure 1b. Moreover, Figs. 3d and 3e show out-of-plane amplitude and phase images, respectively for PVDF/IL samples, with the corresponding images for pure PVDF provided in the supplementary figure 1c. These images were obtained over a scan area of 20×20 μm in the virgin state of the film. The PFM amplitude represents the piezoelectric displacement of the sample when subjected to an AC voltage, while the PFM phase specifies the orientation of polarization. The observed weak contrast regions suggest a low piezoelectric response, possibly due to the lack of the polar β phase in the

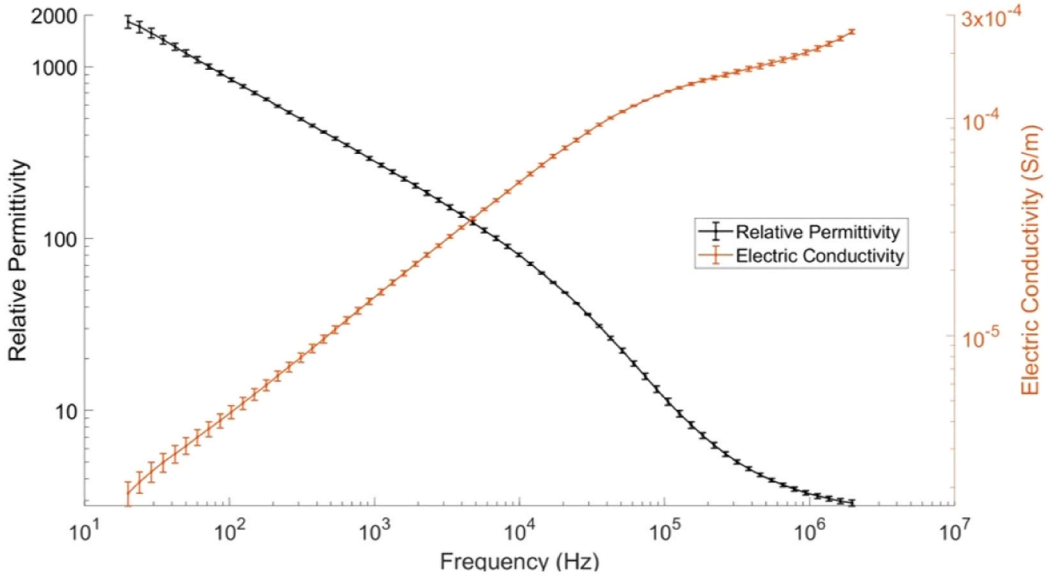

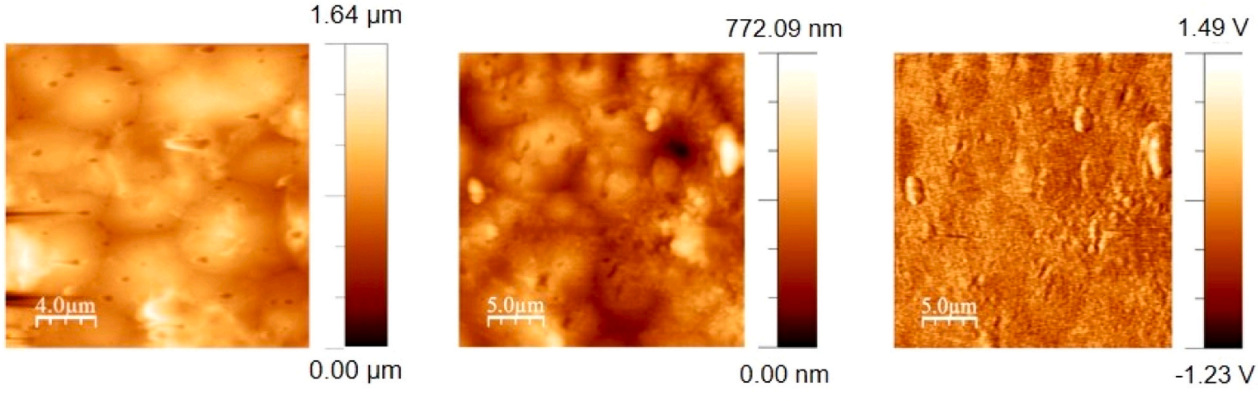

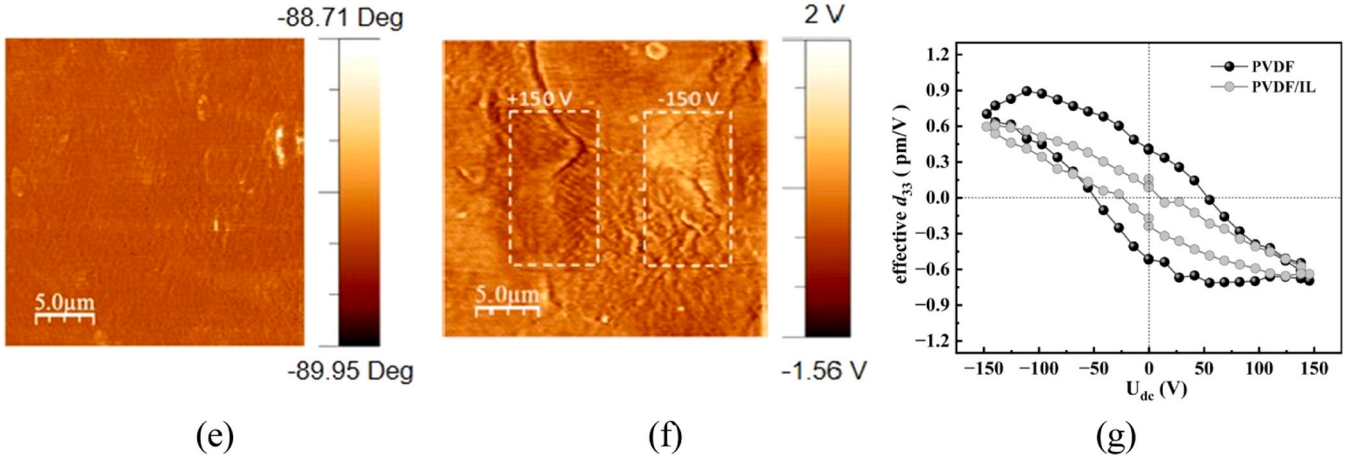

Fig. 3. Electrical and piezoelectric characterization: (a) Relative permittivity and electric conductivity of the PVDF/IL actuators as a function of frequency; (b) AFM topography image of the PVDF/IL film; (c) PFM Topography; (d) Out-of-plane amplitude (A*cosθ); (e) Out-of-plane phase images; (f) PFM amplitude image after applying ±150 V to create artificial domains; and (g) Piezoresponse hysteresis loop obtained by PFM. Error bars in the first figure represent the standard deviation of relative permittivity (black line) and electric conductivity (orange line).

scanned region. Further investigations were performed by applying a DC bias voltage of ±150 V to the tip, effectively inducing microscale tip-induced poling as a means of artificially writing domains. As seen in Fig. 3f, opposite bright and dark contrasts were observed, though with some instability which can be attributed to the higher conductivity of these films. This becomes more apparent when compared to the results for pure PVDF samples, as shown in the supplementary figure 1d.

To further study the local piezoelectric response behaviour, we investigated the hysteresis loops on the PVDF/IL and pure PVDF films (Fig. 3g) using a cantilever tip. These loops were obtained in pulse mode by sweeping the DC bias voltage (U_{dc}) between ±150 V. The results confirm a negligible difference in the ferroelectric characteristics of the film at the nanoscale, with coercive voltages of 55 V for PVDF and 25 V for PVDF/IL, respectively. This reflects only a marginal variation in the d_{33} coefficient values, approximately 0.8 pm/V for PVDF and 0.6 pm/V for PVDF/IL.

Infrared spectroscopy also confirms that the presence of IL leads to a higher percentage of electroactive phase. Supplementary figure 2 shows the FTIR-ATR analysis of PVDF samples with and without IL. Despite similar transmittance (%T) values at 840 cm^{-1} (corresponding to EA phases), a more subtle peak at 766 cm^{-1} (typical of non-EA phases) suggests a higher EA phase content: 80 % in PVDF/IL samples compared to 69 % in PVDF samples, as determined by Beer- Lambert law.

The experimental setup used to characterise the displacement of the

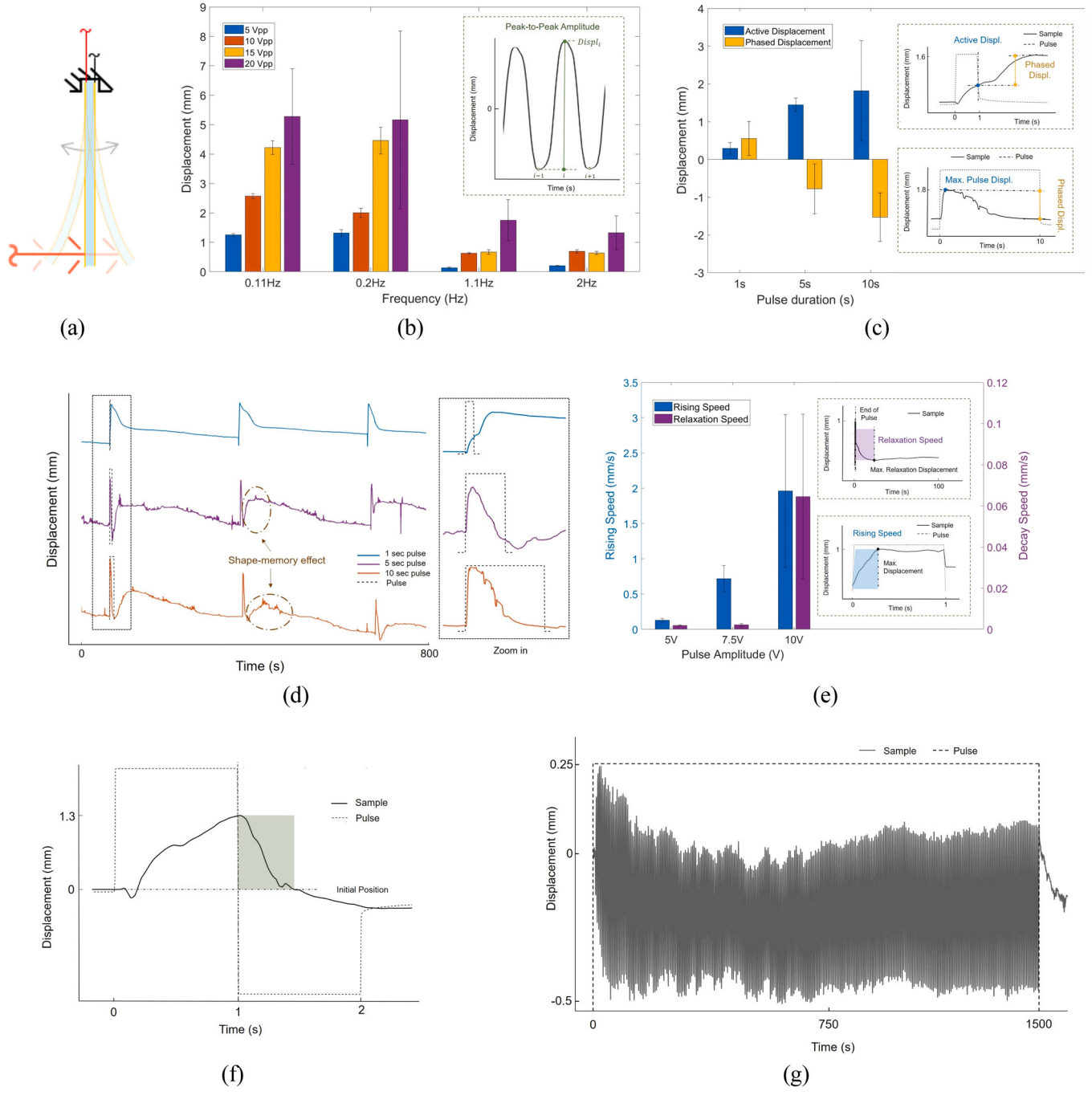

Fig. 4. Electromechanical analysis of the PVDF/IL cantilever beam: (a) Experimental setup; (b) Displacement for sinusoidal input; (c) Displacement for different pulse durations, highlighting active and phased displacements; (d) Typical displacement behavior for square pulses; (e) Rising and relaxation speeds; (f) Reversal motion speed with bipolar pulse stimulation; (g) Cyclic test with a sine wave.

PVDF-IL samples is shown in Fig. 4a. Fig. 4b shows the mean sinusoidal displacement results, investigating the effect of altering input voltage and frequency. In general, higher voltages result in greater peak displacements across all tested frequencies. This is because higher voltages induce stronger polarization, leading to increased displacement, where lower frequencies allow the samples sufficient time to respond due to their relatively slower motion. However, the peak displacement at 20 V_{pp} decreases at higher frequencies because faster frequency induces more rapid polarization changes, limiting the sample's response. Supplementary Videos S1 and S2 show typical displacements for high and low frequencies, 2 Hz and 0.02 Hz, respectively, while actuating with 15 V.

Supplementary material related to this article can be found online at doi:10.1016/j.sna.2024.116038.

A comparison of the electromechanical response of our IL/PVDF film with other PVDF-based piezoelectric actuators with a high electroactive phase, highlights the role of IL in reducing the required input voltage for achieving greater displacement. For example, in a previously published study [18] involving P(VDF-TrFE) copolymer with similar dimensions (25×5 mm) and thickness (≈50 μm) subjected to a comparable frequency (≈1 Hz), a displacement of 0.8 mm was achieved with a sinusoidal input. In contrast, our IL/PVDF film achieved a displacement of 0.67 mm, but required a much lower electric field (0.25 MV m^{-1} compared to 50 MV m^{-1} in the P(VDF-TrFE) study) to achieve comparable displacement performance.

Fig. 4c shows the displacement response of the film under pulse input. It shows active displacement, denoted as the highest displacement achieved by the sample during the pulse, and phased displacement, denoted as the rising displacement after the end of the pulse (as a positive displacement) or the relax- ing displacement during the pulse after the maximum position (as a negative displacement). The results show greater active displacements for higher pulse duration. Exposing the soft actuators to different pulse durations leads to distinct behaviours: with shorter pulse durations (e.g. 1 s), the samples continued to rise after the end of the pulse, achieving a post-pulsed displacement higher than the one achieved during the pulse - see the top inset graph from the typical displacement result in shorter pulse duration. This could be attributed to the presence of IL in the PVDF network, partially through increasing hysteresis [32], which is associated with response delay and remnant polarization [33]. Moreover, it boosts ε' leading to increased energy storage during the pulse duration [31].

In contrast, longer pulse durations lead to a decrease of displacement immediately after reaching the maximum active displacement (Fig. 4c, bottom inset). In this study, the loss increases with the pulse duration. The observed negative phased displacement could be attributed to the dielectric loss, wherein the polarization can not be sustained. The presence of IL amplifies this dielectric loss, since the σ_{AC} increases with its addition and it is related to low IL density [22]. Moreover, compared to other phases (such as α), the β phase is associated with greater dielectric loss [34]. Fig. 4d compares the displacement behaviour of three different samples when subjected to different pulse durations with all data filtered to minimise noise. The comparison between raw and filtered curves is detailed in the supplementary material (supplementary figure 3).

For the 5 s and 10 s pulses, a different phenomenon is observed. After the end of the pulse, and the relaxation of the actuators, they show a secondary rise to a new peak before gradually returning to their initial position. This effect is known as the memory effect which can be attributed to the presence of IL that cross-links PVDF [35]. Moreover, the Joule effect provides a complementary explanation, as it leads to an increase in the internal temperature of the samples when current is passing through the film. Therefore, after the pulse, the temperature gradually decreases, which prevents a rapid return to the initial position [36].

Fig. 4e shows the rising and relaxation speeds for pulse amplitudes of 5, 7.5 and 10 V. We did not observe a noticeable response for 2.5 V. Supplementary figure 4 presents the original and filtered curves for each case. Both rising and relaxation speeds show an increase in pulse intensity, which is related to higher polarization. While 10 V pulse resulted in higher rising and relaxation speeds, it also showed higher standard deviation values. Particularly, at 7.5 V, the relaxation speed is notably lower than the rising speed. This disparity is attributed to the positive phase displacement occurring after the pulse ends, which delays the relaxation speed. In such cases, the relaxation speed was calculated by identifying the minimum decay position following this positive phased displacement (supplementary figure 5). When employing a negative pulse to instantly reverse the actuation, as shown in Fig. 4f, the reversal motion speed showed a faster and consistent response of 9.39 ±2.06 mm/s. This suggests that bipolar square pulses could serve as a viable option to ensure a consistent relaxation response for practical applications such as haptic feedback devices.

Fig. 4g shows the results of the cyclic test conducted to evaluate actuation stability under continuous sinusoidal input. This shows no significant deterioration in peak-to-peak amplitude during 300 cycles of a sine wave input at a voltage amplitude of 10 V_{pp} and a frequency of 0.2 Hz.

To quantify the generated force (Figs. 5a and 5b) our experiments showed that the PVDF/IL can compress the spring by 0.31±0.11 mm, which corresponds to 11±3 mN according to the Hooke law. It falls within the typical threshold values for cutaneous touch perception (10–100 mN) as reported by [37], demonstrating its potential use for haptic feedback, especially considering its relatively quicker actuation response compared to the ionic actuators.

3.1. *Finger sleeve design*

Figs. 5c and 5d show the initial design and prototype of the finger sleeve to assess haptic feedback. The sleeve is 3D printed with a flexible thermoplastic polyurethane filament, incorporating two IL/PVDF cantilever beams for force feedback. These actuators are positioned equidistantly from the finger's center, enabling simultaneous and independent feedback application on both sides. This setup offers the flexibility of applying distinct inputs to each side of the finger (left and right). The supplementary Video S3 showcases the prototype in operation, demonstrating its response to a sine input wave. A comprehensive user study will be carried out to evaluate the detectability of the applied force in different scenarios.

Supplementary material related to this article can be found online at doi:10.1016/j.sna.2024.116038.

4. Conclusions and future works

The present study provides a critical analysis of the electromechanical response of a hybrid piezoelectric-ionic film for potential haptic feedback. The inclusion of ionic liquid into the PVDF network offers several advantages: Firstly, it enhances the electroactive phase during the polymerisation process, thereby boosting the piezoelectric effect, as observed in our sinusoidal displacement studies. Additionally, the addition of the IL reduces the required input actuation voltage, although it becomes prone to failure at voltages higher than 20 V peak to peak. The addition of IL also lowers the Young's modulus of the actuator, resulting in greater displacement. The addition of ionic liquid also causes the electrical parameters, σ_{AC} and ε', to vary significantly with frequency, which leads to higher dielectric loss and energy storage at specific frequencies. Moreover, it increases hysteresis in PVDF/IL piezoelectric responses. These effects result in phased displacement, which could make the control of these hybrid actuators more challenging. Nevertheless, using a shorter input pulse with reversed pulsing for active relaxation can offer a more stable solution.

Further studies on the type of ionic liquid and optimization of the structure and fabrication process are necessary to fully comprehend their electromechanical effect in the hybrid design for optimising

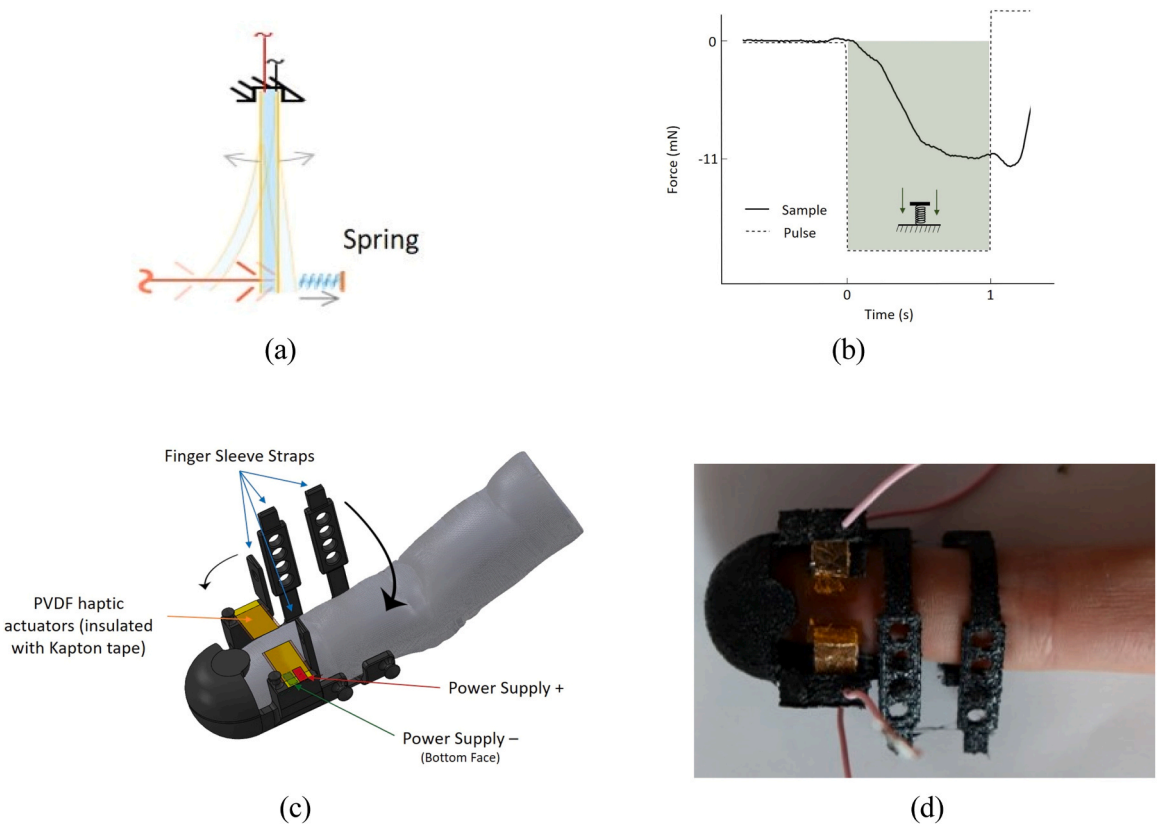

Fig. 5. Force measurement for haptic feedback: (a) Set-up for force measurement; (b) Force result achieved from the compression of the spring. (c) Finger sleeve design; (d) Photo of the fabricated sleeve.

actuation performance. Furthermore, user-studies are essential to assess the feasibility of using this technology for haptic feedback.

CRediT authorship contribution statement

Rui M.R. Pinto: Writing – review & editing, Investigation. **K.B. Vinayakumar:** Writing – review & editing, Investigation. **António Diogo André:** Writing – review & editing, Writing – original draft, Methodology, Investigation, Formal analysis, Conceptualization. **Igor Bdikin:** Writing – original draft, Writing - review & editing, Investigation. **Indrani Coondoo:** Writing – review & editing, Investigation. **Majid Taghavi:** Writing – review & editing, Supervision, Resources, Methodology, Investigation, Conceptualization. **Pedro Martins:** Writing – review & editing, Resources, Investigation, Conceptualization.

Declaration of Competing Interest

The authors declare that they have no known competing financial interests or personal relationships that could have appeared to influence the work reported in this paper.

Acknowledgements

Antoónio Diogo André (A.D.A) gratefully acknowledges funding from FCT, Portugal, under grant SFRH/BD/147807/2019 (https://doi.org/10.54499/SFRH/BD/147807/2019) and from European Union (UE) under Erasmus+ 2019 Credit Mobility project (2019–1-PT01-KA103–060090) and WORK4ALL 3 project (2020–1-PT01-KA103–077725). Pedro Martins (P.M.) gratefully acknowledges funding from project UIDB/50022/2020 financed by FCT, through INEGI, under LAETA. Indrani Coondoo (I.C.) and Igor Bdikin (I.B) acknowledge funding through the FCT project "MultiFlex" EXPL/CTM-CTM/0687/2021 (http://doi.org/10.54499/EXPL/CTM-CTM/0687/2021). I. C. would also like to acknowledge financial assistance by national funds (OE), through FCT, I.P., Portugal through DL57/2016/CP1482/CT0048 (https://doi.org/10.54499/DL57/2016/CP1482/CT0048). I.B. also acknowledges the Project "Agenda ILLIANCE" [C644919832–00000035 — Project no. 46], financed by PRR – Recovery and Resilience Plan under the Next Generation EU from the European Union. Majid Taghavi (M.T.) acknowledges Imperial College Research Fellowship.

Appendix A. Supporting information

Supplementary data associated with this article can be found in the online version at doi:10.1016/j.sna.2024.116038.

Data Availability

Data supporting this study are openly available from Zenodo at https://doi.org/10.5281/zenodo.14052677

References

[1] Jimin Gu Junseong Ahn, Chankyu Han Jungrak Choi, Jaeho Park Yongrok Jeong, Yong Suk Oh Seokjoo Cho, Morteza Amjadi Jun-Ho Jeong, Inkyu Park, A review of recent advances in electrically driven polymer- based flexible actuators: smart materials, structures, and their applications, Adv. Mater. Technol. 7 (11) (2022).
[2] Vivek Mishra, Shubham Pandey, Simran Aggarwal, Electroactive Polymers in Industry, CRC Press, March, 2022, pp. 271–298.
[3] Siegfried Bauer, Electroactive polymers for healthcare and biomedical applications. Yoseph Bar-Cohen, editor, Electroactive Polymer Actuators and Devices (EAPAD), SPIE, 2017, p. 2017.
[4] António Diogo Andé, Pedro Martins, Exo supportive devices: summary of technical aspects, Bioengineering 10 (11) (2023) 1328.
[5] Yang Cao, Jingyan Dong, Fabrication and self-sensing control of soft electrothermal actuator, Procedia Manuf. 48 (2020) 43–48.

[6] Terence Yan King Ho Ankit, Nirmal Amoolya, Rameshchandra Kulkarni Mohit, Dino Accoto, Mathews Nripan, Soft actuator materials for electrically driven haptic interfaces, Adv. Intell. Syst. 4 (2) (2021).
[7] Yoseph Bar-Cohen, 2004, Actuators as Artificial Muscles: Reality, Potential, and Challenges, Second Edition (SPIE Press Monograph Vol. PM136). SPIE Publications, 2004.
[8] Yoseph Bar-Cohen, Iain A. Anderson, Electroactive polymer (eap) actuators—background review. Mech. Soft Mater. 1 (1) (2019).
[9] R. Heydt Refreshable braille display based on electroactive polymers. 2003.
[10] Kailiang Ren, Sheng Liu, Minren Lin, Yong Wang, Q.M. Zhang, A compact electroactive polymer actuator suitable for refreshable braille dis- play, Sens. Actuators A: Phys. 143 (2) (May 2008) 335–342.
[11] John G. Hardy, David J. Mouser, Netzahualcóyotl Arroyo-Currás, et al., Biodegradable electroactive polymers for electrochemically- triggered drug delivery, J. Mater. Chem. B 2 (39) (2014) 6809–6822.
[12] N. Soin, D. Boyer, K. Prashanthi, S. Sharma, A.A. Narasimulu, J. Luo, T.H. Shah, E. Siores, T. Thundat, Exclusive self-aligned β-phase pvdf films with abnormal piezoelectric coefficient prepared via phase inversion, Chem. Commun. 51 (39) (2015) 8257–8260.
[13] Kie Yong Cho, Hyunchul Park, Hyun-Ji Kim, Xuan Huy Do, Chong Min Koo, Seung Sang Hwang, Ho Gyu Yoon, Kyung-Youl Baek, Highly enhanced electromechanical properties of pvdf-trfe/swcnt nanocompos- ites using an efficient polymer compatibilizer, 21–29, mar, Compos. Sci. Technol. 157 (2018), 21–29, mar.
[14] Juliana C. Dias, Daniela M. Correia, Carlos M. Costa, Clarisse Ribeiro, Alberto Maceiras, José L. Vilas, Gabriela Botelho, Verónica de Zea Bermudez, Senentxu Lanceros-Mendez, Improved response of ionic liquid-based bending actuators by tailored interaction with the polar fluorinated polymer matrix, Electrochim. Acta 296 (2019) 598–607.
[15] Sheng Liu, Yang Liu, Hulya Cebeci, Roberto Guzmán de Villoria, Jun-Hong Lin, Brian L. Wardle, Q.M. Zhang, High electromechanical response of ionic polymer actuators with controlled-morphology aligned carbon nan- otube/nafion nanocomposite electrodes, Adv. Funct. Mater. 20 (19) (2010) 3266–3271.
[16] Junkao Liu Xuefeng Ma, Jie Deng Shijing Zhang, Yingxiang Liu, Recent trends in bionic stepping piezoelectric actuators for precision positioning: a review. Sens. Actuators A: Phys. 364 (2023) 114830.
[17] Miroslav Král Ricardo Perez, Hannes Bleuler, Study of polyvinylidene fluoride (pvdf) based bimorph actuators for laser scanning actuation at khz frequency range, Sens. Actuators A: Phys. 183 (2012) 84–94.
[18] Tomohito Sekine Yoshinori Shouji, Naoya Ito Keita Ito, Yi-Fei Wang Tatsuya Yasuda, Daisuke Kumaki Yasunori Takeda, Atsushi Miyabo Fabrice Domingues Dos Santos, Fast Shizuo Tokito, response, high-power tunable ultrathin soft actuator by functional piezoelectric material composite for haptic device application. Adv. Electron. Mater. 9 (9) (2023).
[19] Enes Selman Ege, Abdulkadir Balikci, Transparent localized haptics: Utilization of pvdf actuators on touch displays, Actuators 12 (7) (2023) 289.
[20] Fawad Ali, Muammer Koc, 3d printed polymer piezoelectric materials: Transforming healthcare through biomedical applications, Polymers 15 (23) (2023) 4470.
[21] Liuxia Ruan, Xiannian Yao, Yufang Chang, Lianqun Zhou, Gaowu Qin, Xianmin Zhang, Properties and applications of the phase poly(vinylidene fluoride). Polymers 10 (3) (2018) 228.
[22] D.M. Correia, J.C. Barbosa, C.M. Costa, P.M. Reis, J.M.S. Esperança, V. de Zea Bermudez, S. Lanceros-Méndez, Ionic liquid cation size-dependent electromechanical response of ionic liquid/poly(vinylidene fluoride)-based soft actuators, J. Phys. Chem. C. 123 (20) (2019) 12744–12752.
[23] Daniela M. Correia, Carlos M. Costa, Erlantz Lizundia, Roser Sabater I Serra, José A. Gómez-Tejedor, Laura Teruel Biosca, José M. Meseguer- Dueñas, José L. Gomez Ribelles, Influence of cation and anion type on the formation of the electroactive - phase and thermal and dynamic mechanical properties of poly(vinylidene fluoride)/ionic liquids blends, J. Phys. Chem. C. 123 (45) (oct 2019) 27917–27926.
[24] R. Mejri, J.C. Dias, S. Besbes Hentati, M.S. Martins, C.M. Costa, S. Lanceros-Mendez, Effect of anion type in the performance of ionic liquid/poly(vinylidene fluoride) electromechanical actuators, J. Non-Cryst. Solids 453 (2016) 8–15.
[25] Umar Raza, Saewoong Oh, Rassoul Tabassian, Manmatha Mahato, Van Hiep Nguyen, Il-Kwon Oh, Micro-structured porous electrolytes for highly responsive ionic soft actuators, Sens. Actuat. B: Chem. 352 (2022) 131006.
[26] Tian Chen Kai Xiang, Air-working Yanni Wang, ionic soft actuator based on three-dimensional graphene electrode. Mater. Lett. 286 (2021) 129267.
[27] António Diogo André, Ana Margarida Teixeira, Pedro Martins, Influ- ence of dmso non-toxic solvent on the mechanical and chemical properties of a pvdf thin film, Appl. Sci. 14 (8) (2024).
[28] Clarisse Ribeiro, Carlos M Costa, Daniela M. Correia, João Nunes-Pereira, Juliana Oliveira, Pedro Martins, Renato Goncalves, Vanessa F Cardoso, Senentxu Lanceros-Méndez, Electroactive poly(vinylidene fluoride)-based structures for advanced applications, Nature Protocols 13 (4) (2018) 681–704.
[29] D.M. Correia, L.C. Fernandes, N. Pereira, J.C. Barbosa, J.P. Serra, R.S. Pinto, C. M. Costa, S. Lanceros-Méndez, All printed soft actuators based on ionic liquid/ polymer hybrid materials, Appl. Mater. Today 22 (March 2021) 100928.
[30] Xingang Liu, Yinghao Shang, Jihai Zhang, Chuhong Zhang, Ionic liquid-assisted 3d printing of self-polarized β-pvdf for flexible piezoelectric energy harvesting. ACS Appl. Mater. Interfaces 13 (12) (2021) 14334–14341.
[31] Arthur R. Von Hippel, Dielectrics and Waves (Artech House Microwave Library), Artech House Publishers, 1995.
[32] Runkai Zhou, et al., Effects of ionic liquid content on the electrical properties of pvdf films by fused deposition modeling, Materials 17 (1) (2023).
[33] M. Date, T. Furukawa, E. Fukada, Dipolar orientation and hysteresis in polyvinylidene fluoride, J. Appl. Phys. 51 (7) (1980) 3830–3833.
[34] Bao-Wen Li Hexing Liu, Zhonghui Shen Jiayu Chen, Jing Wang Xin Zhang, Ce-Wen Nan, Concurrent enhancement of breakdown strength and dielectric constant in poly(vinylidene fluoride) film with high energy storage density by ultraviolet irradiation, ACS Omega 7 (30) (2022) 25999–26004.
[35] Aoki Kota, Sugawara-Narutaki Ayae, Doi Yuya, Rintaro Takahashi, Structure and rheology of poly(vinylidene difluoride-co-hexafluoropropylene) in an ionic liquid: The solvent behaves as a weak cross-linker through ion–dipole interaction, Macromolecules 55 (13) (2022) 5591–5600.
[36] Gozde Aktas Eken, Metin H. Acar, Pvdf-based shape memory polymers, Eur. Polym. J. 114 (2019) 249–254.
[37] Christian Hatzfeld and Thorsten A. Kern. Engineering Haptic Devices A Beginner's Guide. Springer.

António Diogo André is currently a PhD candidate in Mechanical Engineering at the Faculty of Engineering of University of Porto (FEUP), developing his PhD project in soft piezoelectric materials under the theme "Exoskeleton for Aided-Mobility" at INEGI. During that period, he was a visiting student at Imperial College London between 2022 and 2023. He is the author and co-author of several scientific papers, abstracts in national and international conferences and chapters of books.

Indrani Coondoo is a Research Scientist at the Department of Materials and Ceramics Engineering, University of Aveiro (UA), and CICECO - Aveiro Institute of Materials. She earned her PhD from the Faculty of Technology, University of Delhi (formerly Delhi College of Engineering). Before joining UA, she worked as a postdoctoral researcher at the National Physical Laboratory, India and the University of Puerto Rico, USA. Her research focuses on engineered multifunctional materials, including ferroelectrics and piezoelectrics (polymers, ceramics, and thin films). She aims to advance materials for energy conversion, energy storage, and multi-caloric cooling applications. Additionally, she is exploring additive manufacturing (3D printing) techniques to develop materials/systems for next-generation sensors, transducers, and energy harvesters. She has authored 70 research papers in international peer-reviewed journals and has presented her work at around 50 conferences. She is also the co-inventor of a U.S. patent.

Igor Bdikin graduated in Physics from the Physics Department of the Kazan State University in 1989 and completed a PhD degree in Solid State Physics from the Institute of Solid State Physics, Russia in 1999. From 1999–2003 he worked in the Laboratory of Structural Research of the Institute of Solid State Physics, Russia as a researcher. From 2003–2009 he worked in Department of Ceramics and Glass Engineering, University of Aveiro, Portugal as a postdoctoral fellow. Since 2009 he is employed as a researcher in the Centre for Mechanical Technology Automation (TEMA) in the University of Aveiro, Portugal. His scientific activities & collaborations with several R&D groups and industries have resulted in more than 250 publications, 5 book chapters & 30 conference proceedings.

Vinaya Kumar K B earned his PhD from the Indian Institute of Science (IISc), India, where he specialized in the design and development of microsystems for a minimally invasive wearable insulin delivery system (microneedles and micropumps). In December 2015, He joined Cornell University, USA, as a Postdoctoral Associate, he made significant contributions to the field by working **on miniature ion accelerators utilizing the MEMS approach.** In July 2018 he joined INL Portugal to work on vacuum electronics, printed electronics and sensors for medical applications. Currently, he is working at BITS Pilani Goa campus as an Assistant Professor.

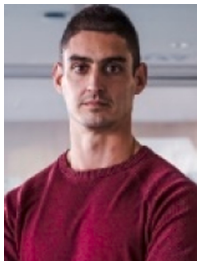

Rui M. R. Pinto is a Research Engineer at INL since 2021, where he has been involved in optimizing inkjet heads, printing processes, and gas sensing systems. He received his Ph.D. degree in biotechnology and biosciences from Instituto Superior Técnico, University of Lisbon, in 2020. His thesis was on the development of thin-film silicon MEMS for mass sensing and biosensing applications. His other interests include prototyping, micro and nanofabrication, micromechanical devices, electronic instrumentation, microscopy, surface functionalization, microfluidics, and biosensing.

Dr. Pedro Martins has researched the mechanics and structure of female soft biological tissues and medical implants since beginning his PhD in 2004. His doctoral thesis focused on the nonlinear mechanical behavior of female pelvic tissues, and he developed techniques for experimental analysis and data fitting. Collaborating with researchers from Spain and Brazil, he created models for the mechanical behavior of vaginal tissues and pelvic floor implants. He led the Biomechanics Laboratory at INEGI (Portugal) until 2022, with contributions in soft robotics and bioprinting of scaffolds for breast tissue regeneration. Currently, he is an ARAID researcher at I3A/UNIZAR (Spain), he explores advanced AI techniques, such as Physics-Informed Graph Neural Networks, applied to Digital Human Twins and structural mechanics problems.

Majid Taghavi is an Associate Professor at Queen Mary University of London and a Research Fellow at Imperial College London, where he leads an interdisciplinary research group focused on Soft Robotic Transducers. He has also worked at SoftLab, University of Bristol, UK, and IIT@Sant'Anna, Italy. Majid has pioneered several artificial muscle, variable stiffness, energy harvesting, and self-powered sensing technologies.